PHYSICAL REVIEW B, VOLUME 64, 073304

First- and second-order Raman scattering in nanocrystalline silicon

Puspashree Mishra* and K. P. Jain
Department of Physics, Indian Institute of Technology, Delhi, Hauz Khas, New Delhi 110016, India
(Received 20 February 2001; published 26 July 2001)

Confinement effects on first-order and second-order Raman scattering in nanocrystalline silicon are presented. The average dimension of the nanocrystals has been determined by an analysis of the first-order Raman spectra using the phenomenological phonon confinement model. The second-order acoustic bands 2LA and 2TA do not seem to be influenced by confinement effects and are similar to those in the bulk. The second-order optic bands are broadened and shifted in comparison to those in the bulk. The ratio of the integrated intensities $I(2\mathrm{TO})_{\mathrm{int}}/I(\mathrm{TO})_{\mathrm{int}}$ depends upon the nanocrystal size and varies between the crystalline and amorphous limits.

DOI: 10.1103/PhysRevB.64.073304 PACS number(s): 78.30.−j, 78.67.−n, 78.66.Jg, 63.22.+m

I. INTRODUCTION

Quantum confined semiconductors have tremendous potential for future novel electronic and optical properties and exhibition of new quantum phenomena.[1,2] Discovery of room-temperature photoluminescence[3] from Si nanocrystals, for example, has initiated a lot of interest worldwide for potential application in optoelectronic devices. Confinement effects in reduced dimension systems lead to major modifications of the electronic, linear and nonlinear optical and vibrational properties. These contain information about many parameters, which are essential to understand semiconductor device operation as well as the physics of the materials themselves. Raman spectroscopy is an excellent nondestructive optical tool to study the change in the vibrational properties. For example, line shape analysis of the first-order Raman spectrum can give important information about the crystalline, amorphous or nanocrystalline nature of the material. The average dimension of the nanocrystals can also be ascertained by analyzing the line shape of the first-order Raman spectrum.[4,5]

In the second-order Raman scattering process, two phonons of equal and opposite momentum participate and produce either line or broad continuous spectrum. Zone edge phonons, which appear only in higher-order Raman scattering, correspond to large wave vectors and are sensitive to short-range disorder. For partially disordered systems, this results in the damping of the two phonon Raman amplitude.[6,7] The nature of a material, such as crystalline or amorphous, can therefore be ascertained by analyzing the higher-order phonons as well. First-order Raman spectrum of nanocrystalline silicon has been studied extensively.[8–10] However, there have been very few reports of higher-order Raman spectrum in silicon nanocrystals because of their weak intensity. Munder *et al.*[11] and Gregora *et al.*[12] studied the multiphonon processes in porous silicon and concluded that the multiphonon processes are surface assisted.

The purpose of this paper is to study the effects of confinement on the first- and second-order Raman scattering in Si nanocrystals. The Si nanocrystals used in the present study, were fabricated by cw laser annealing of a-Si:H. The most probable dimension of the nanocrystallites was determined by an analysis of the first-order Raman spectra using the phenomenological phonon confinement model.[4,5] The position and width of the second-order optic bands are compared with those of the bulk silicon. These bands are broadened and shifted in comparison to the bulk. A comparative study of the integrated intensity ratio of the second and first-order Raman peaks in bulk, a-Si and the nanocrystalline silicon indicates that the ratio of the integrated intensities $I(2\mathrm{TO})_{\mathrm{int}}/I(\mathrm{TO})_{\mathrm{int}}$ depends upon the nanocrystal size and varies between the crystalline and amorphous limits. The second-order acoustic bands are found to be uninfluenced by the confinement effects.

II. EXPERIMENTAL PROCEDURE

Raman scattering experiments were performed in the back-scattering geometry configuration by using the 5145-Å line of an argon-ion laser, a RAMANOR double monochromator and photon counting electronics. The Si nanocrystals used for the present study were fabricated by cw laser annealing of a-Si:H samples of thickness 1100 and 5000 Å grown on quartz substrates maintained at 250 °C. The hydrogen concentration in the films was roughly 8%. Controlled cw laser annealing of the a-Si:H samples on diffraction limited spots of 40 μm was done by employing an argon-ion laser and optimizing the power density and the exposure time of the laser. The exposure time was controlled by an electronic shutter. Uniform annealing over an area of 2 mm $\times$2 mm was also achieved by scanning the argon-ion laser over the sample and using a X-Y translator and optimizing the annealing power density and the scan speed of the translator. The incident power of the laser during Raman experiments was kept low to avoid distortion of the spectra due to laser heating. The monochromator was calibrated properly by noting down the positions of the plasma lines before recording each spectrum. The spectral resolution for the measurement of first-order and second-order Raman spectra was 1 and 3.5 cm^{-1}, respectively.

III. RESULTS AND DISCUSSION

Figure 1 shows the gradual modification of the first-order Raman spectra of the a-Si:H film on quartz substrate with increasing power density of the annealing laser beam. The Raman spectrum of the unannealed a-Si:H film is given in Fig. 1(a). This spectrum is a measure of the density of vibra-

 ©2001 The American Physical Society

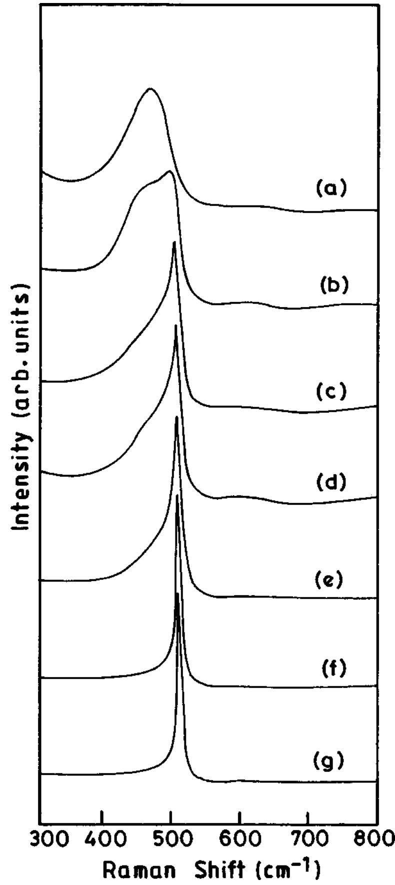

FIG. 1. The room temperature Raman spectra of a-Si:H film annealed with a cw argon ion laser ($\lambda = 5145$ Å) and power densities (b) 18.05 Kw/cm^2, (c) 19.9 Kw/cm^2, (d) 21.7 Kw/cm^2,(e) 23.5 Kw/cm^2, (f) 25.3 Kw/cm^2, (g) 28.9 Kw/cm^2, respectively. The exposure time was fixed at 1/125 secs. (a) shows the Raman spectrum of the unannealed film.

tional states due to loss of long-range order and translational symmetry in amorphous materials. The most prominent feature observed is the TO band at 475 cm^{-1} with a full width at half maximum (FWHM) of 80 cm^{-1}. Figures 1(b)–1(g) show the Raman spectra of the a-Si:H sample annealed using a 40 μm focussed spot of a cw argon-ion laser of wavelength 514.5 nm and power densities ranging from 18.05 to 28.9 Kw/cm^2. The exposure time of the annealing laser was kept fixed at 1/125 s by means of an electronic shutter.

There is no change in the Raman line shape of the a-Si:H film when the annealing power density is changed from a very low value to about 18.05 Kw/cm^2. At an annealing power density of 18.05 Kw/cm^2, a shoulder at 503 cm^{-1} corresponding to nanocrystalline silicon emerges, which overlaps the broad spectrum of amorphous silicon. This peak shifts to 513.5 cm^{-1} as the power density is increased to 28.9 Kw/cm^2. The overall line shape becomes narrower and more symmetric as the annealing power density increases. Similar variation of the Raman line shape is also observed with increasing exposure time and constant power density of the annealing laser beam. Conventional furnace annealing can also produce results similar to cw laser annealing used in the present study. Massie *et al.*[13] have studied the effect of standard furnace annealing on an a-Si:H/a-Ge:H multilayer film, and have measured the Raman spectra for different annealing temperatures. We observe that the Raman spectrum obtained for 600 °C standard furnace annealing by Massie *et al.*[13] closely resembles our Raman spectrum shown in Fig. 1(b) (Annealing power density: 18.05 Kw/cm^2), in which a peak corresponding to the nanocrystals emerges overlapping the amorphous spectrum.

The average dimension of the Si nanocrystals was found out using a phenomenological phonon confinement model.[4,5] According to this, confinement or localization of phonons in nanocrystals results in uncertainty in the phonon momentum, allowing phonons with $q \neq 0$ to contribute to the Raman spectrum, thus leading to softening and asymmetric broadening of the first-order Raman spectrum. The Raman intensity is therefore given by

$$I(\omega) = \int_q \frac{|C(0,q)|^2}{\{[\omega - \omega(q)]^2 + (\Gamma_0/2)^2\}} d^3q, \tag{1}$$

where $I(\omega)$ is the intensity of the Raman spectrum, $\omega(q)$ is the phonon-dispersion of the bulk material, Γ_0 is the natural linewidth, and $C(0,q)$ is the Fourier coefficient of the phonon confinement function. We have chosen a Gaussian weighting function with a value of $\exp(-4\pi^2)$ at the boundary of the crystallites corresponding to a rigid confinement of the phonons in the nanocrystal (amplitude≈ 0 at the boundary).

Therefore, the first-order Raman spectrum $I(\omega)$ is given by

$$I(\omega) = \int_0^1 \frac{\exp(-q^2 L^2/4a^2)}{\{[\omega - \omega(q)]^2 + (\Gamma_0/2)^2\}} d^3q. \tag{2}$$

Here, q is expressed in units of $2\pi/a$, a is the lattice constant (5.430 Å) of silicon and Γ_0 is the linewidth of the silicon LO phonon in C-Si bulk ($\sim$4 cm^{-1} including instrumental contributions). The dispersion $\omega(q)$ of the LO phonon is given by the relation[14]

$$\omega^2(q) = A + B\cos(\pi q/2), \tag{3}$$

where $A = 1.714 \times 10^5$ cm^{-2} and $B = 1.000 \times 10^5$ cm^{-2}.

Line-shape fitting of the experimental results to Eqs. (2) and (3) was done to determine the average dimensions, care being taken to separate out the amorphous background from the spectra. The contribution from the tensile strain due to different thermal expansion coefficients of the quartz substrate and the Si film was also considered. The details of the annealing procedure and these influencing factors, have been discussed elsewhere.[15] From the line shape analysis it was found that the most probable dimension of nanocrystals was in the range of 2–7 nm, which depends upon the annealing power density.

The growth of second-order bands was monitored from the amorphous to the nanocrystalline phase of the laser annealed a-Si:H sample. Figure 2 displays the growth of second-order bands with variation in the power density of the annealing beam. Very small nanocrystals were not studied due to the weak intensity of the second-order scattering. Fig-

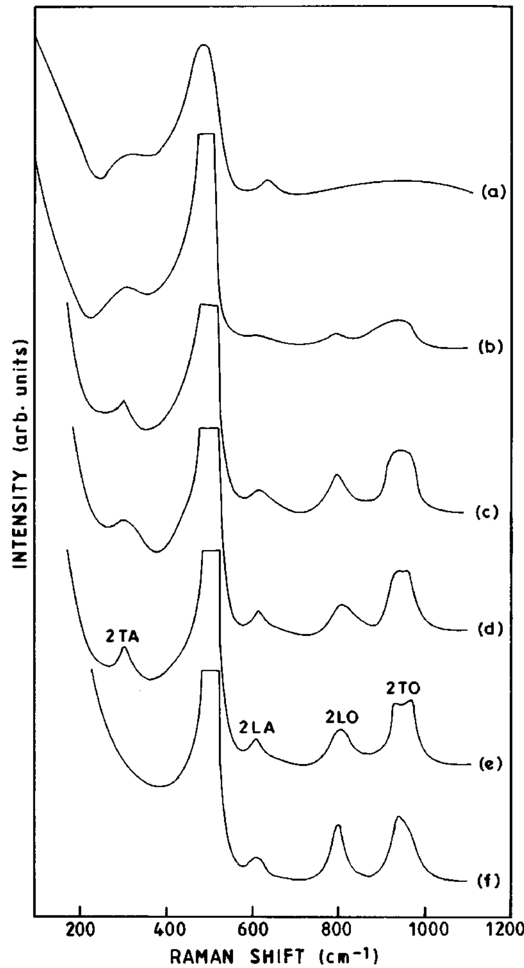

FIG. 2. Growth of second-order bands in a-Si:H sample annealed with a CW argon ion laser ($\lambda = 5145$ Å) and power densities b) 23.5 Kw/cm^2 c) 25.3 Kw/cm^2 d) 28.9 Kw/cm^2 e) 32.5 Kw/cm^2 f) 36.1 Kw/cm^2, respectively, at an exposure time of 1/125 secs. a) shows the Raman spectrum of the unannealed spectra.

ure 2(a) shows the Raman spectrum of the unannealed a-Si:H film. It is clear that all the second-order bands such as 2TA, 2LA, 2TO, and 2LO, which are seen in the Raman spectrum of the crystalline silicon are also visible in the laser-annealed nanocrystalline samples. The absolute intensity of the second-order bands increase with an increase in the size of the nanocrystals and the power density of the annealing beam.

Second-order optic bands in the nanocrystalline silicon samples were found to be shifted and broadened in comparison to the corresponding bands in the bulk crystalline silicon. Details of the FWHM and the position of the 2TO bands are given in Table I. The shoulder at 940 cm^{-1} in the bulk, which is identified as the two TO-phonon overtone at W,[16] appears at 930 cm^{-1} in the nanocrystalline sample of average dimension 5 nm and shifts towards the bulk position as the size increases. Further, the shoulder at 975 cm^{-1} in the bulk, corresponding to two 2TO-phonon overtone scattering from the critical point at L, appears at 965 cm^{-1} in the sample of average dimension 5 nm and again shifts towards the bulk position as the dimension increases. Furthermore, the width

TABLE I. Position of 2TO(W) and 2TO(L), FWHM of the 2TO band, corresponding dimensions of the nanocrystals and annealing power density. The corresponding positions and widths in C-Si are also given.

Power density (Kw/cm^2)	L (nm)	2TO(W)	2TO(L)	FWHM (cm^{-1})
25.3	5	930	965	76
28.9	6	935	965	76
32.5	7	935	970	72
36.1	7	940		68
C-Si		940	975	60

of the 2TO band in the nanocrystalline sample (5 nm) is found to be about 16 cm^{-1} larger than that of crystalline silicon. The 2TO band narrows as the size of the nanocrystals become larger. It is clear from these results that the 2TO band is affected by confinement effects and shifts towards lower frequency and becomes broader as the dimension of the nanocrystals decreases.

As far as the absolute intensity of the 2TO band is concerned, the 2TO band seems to be damped in comparison to those in the bulk. Brodsky *et al.*[17] calculated the ratio of the integrated intensities of the TO and 2TO peaks in a-Si and compared them with those in bulk silicon. They found that the ratio of the second-order to first-order intensities is higher in a-Si than in C-Si. The integrated intensity of 2TO band normalized with respect to the integrated intensity of the TO peak was found to be 0.25 in a-Si and 0.1 in C-Si. Similar ratios for the integrated and peak intensities of nanocrystalline silicon were determined. Figure 3 shows the variation of the $I(2\mathrm{TO})_{\mathrm{int}}/I(\mathrm{TO})_{\mathrm{int}}$ with nanocrystal size and annealing power density. It is clear that the ratio of the peak and the integrated intensities depends on the nanocrystal size and varies between the amorphous and crystalline limits. For larger nanocrystals (7 nm), this ratio is almost equal to the bulk value.

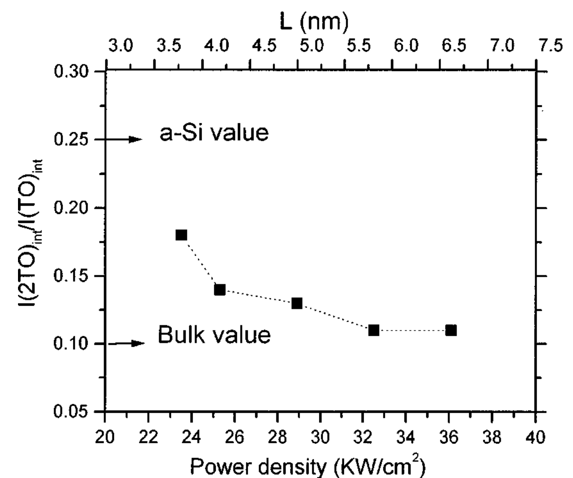

FIG. 3. Variation of integrated intensity ratio of the 2TO and TO peaks with annealing power density for the nanocrystals. The dashed curve is a guide to the eye. Corresponding values in the bulk and amorphous silicon are indicated.

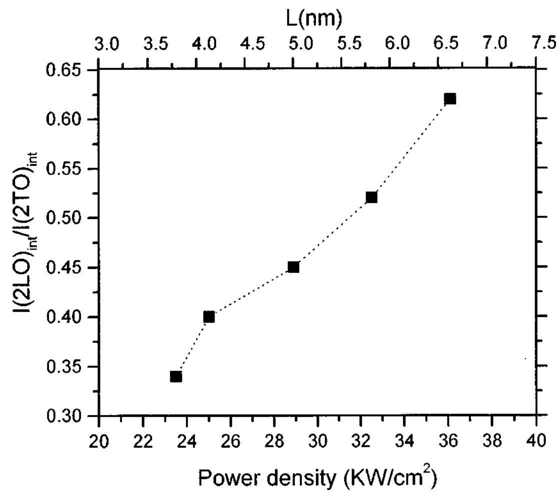

FIG. 4. Variation of integrated intensity ratio of the 2LO and 2TO peaks with annealing power density for the nanocrystals. The dashed curve is a guide to the eye.

The 2LO band in the nanocrystalline silicon is also broadened and shifted towards lower frequency *vis-à-vis* those in the bulk. This band appears at 800 cm^{-1} for $L=5.7$ nm in contrast to the 2LO band at 825 cm^{-1} in C-Si. The 2LO band narrows down and shifts towards the bulk position as the annealing power density and the size of the nanocrystal increases. The variation of the intensity of the 2LO band with increasing annealing power density and dimension of nanocrystals is interesting. It is seen from Fig. 2 that the intensity of the 2LO band increases with increasing annealing power densities and ultimately becomes comparable to the 2TO band intensity. This is in sharp contradistinction to the 2LO intensity in crystalline silicon, which is negligible to the 2TO intensity. Figure 4 shows the variation of the ratio of the integrated intensity of 2LO and 2TO for nanocrystalline silicon. The high scattering efficiency for the 2LO band in nanocrystalline silicon is not well understood and is an open question and could be related to some kind of disorder during the high temperature annealing process.

Turning to the acoustic bands, it was found that they were not much influenced by confinement effects. The positions of the 2TA and 2LA bands were at 302 and 610 cm^{-1}, which are the same as those in the bulk. Negligible frequency shift of higher order acoustic bands was also observed in porous silicon.[12]

IV. CONCLUSION

Nanocrystalline silicon samples were prepared by the cw laser annealing process. The average dimension of the nanocrystals was determined from an analysis of the first-order Raman spectra using a phenomenological phonon confinement model. Second-order optic bands were found to be shifted and broadened in comparison to those in the bulk. The position and the width of these bands approach those in the bulk as the average dimension increases. The ratio of the integrated intensities $I(2\mathrm{TO})_{\mathrm{int}}/I(\mathrm{TO})_{\mathrm{int}}$ of nanocrystasls were found to lie in between those for crystalline and amorphous silicon. Both these ratios are higher than those in the bulk and approach the bulk value with increasing dimension. The scattering efficiency of the 2LO band was found to be higher than that in crystalline silicon. The intensity of this band increases with increasing annealing power density and ultimately becomes comparable to that of the 2TO band. The anomalous behavior of the 2LO intensity in nanocrystalline silicon is not well understood and may be related to some kind of disorder due to high temperature annealing process. The second-order acoustic bands were found to be uninfluenced by confinement effects.

*Present address: Department of Communications and Systems, University of Electro-Communications, 1-5-1 Chofugaoka, Chofu-Shi, Tokyo, 182-8585, Japan

[1] H. Haug and S. W. Koch, *Quantum Theory of the Optical and Electronic Properties of Semiconductors* (World Scientific, Singapore, 1993).
[2] F. Henneberger, S. Schmitt-Rink, and E. O. Gabel, *Optics of Semiconductor Nanostructures* (Academic Verlag, Berlin, 1993).
[3] L. T. Canham, Appl. Phys. Lett. **57**, 1046 (1990).
[4] H. Richter, Z. P. Wang, and L. Ley, Solid State Commun. **39**, 625 (1981).
[5] I. H. Campbell and P. M. Fauchet, Solid State Commun. **58**, 739 (1986).
[6] K. P. Jain, A. K. Shukla, S. C. Abbi, and M. Balkanski, Phys. Rev. B **32**, 5464 (1985).
[7] K. P. Jain, A. K. Shukla, R. Ashokan, S. C. Abbi, and M. Balkanski, Phys. Rev. B **32**, 6688 (1985).
[8] E. Bustarret, M. A. Hachicha, and M. Brunel, Appl. Phys. Lett. **52**, 1675 (1988).
[9] Z. Sui, P. P. Leong, I. P. Herman, G. S. Higashi, and H. Temkin, Appl. Phys. Lett. **60**, 2086 (1992).
[10] M. Fujii, Y. Kanzawa, S. Hayashi, and K. Yamamoto, Phys. Rev. B **54**, R8373 (1996).
[11] H. Munder, C. Andrzejak, M. G. Berger, U. Klemradt, H. Luth, R. Herino, and M. Ligeon, Thin Solid Films **221**, 27 (1992).
[12] I. Gregora, B. Champagnon, L. Saviot, and Y. Monin, Thin Solid Films **255**, 139 (1995).
[13] S. T. Massie, C. J. Doss, R. Zallen, D. Pang, P. Wickboldt, and W. Paul, in *Proceedings of the 22nd International Conference on the Physics of Semiconductors*, edited by D. J. Lockwood (World Scientific, Singapore, 1995), pp. 2709.
[14] Y. Kanemitsu, H. Uto, Y. Masumoto, T. Matsumoto, T. Futagi, and H. Mimura, Phys. Rev. B **48**, 2827 (1993).
[15] Puspashree Mishra and K. P. Jain, Phys. Rev. B **62**, 14 790 (2000).
[16] Paul A. Temple and C. E. Hathaway, Phys. Rev. B **7**, 3685 (1973).
[17] M. H. Brodsky, Manuel Cardona, and J. J. Cuomo, Phys. Rev. B **16**, 3556 (1977).